Development 134, 1323-1335 (2007) doi:10.1242/dev.02812

H^+ pump-dependent changes in membrane voltage are an early mechanism necessary and sufficient to induce *Xenopus* tail regeneration

Dany S. Adams, Alessio Masi and Michael Levin*

In many systems, ion flows and long-term endogenous voltage gradients regulate patterning events, but molecular details remain mysterious. To establish a mechanistic link between biophysical events and regeneration, we investigated the role of ion transport during *Xenopus* tail regeneration. We show that activity of the V-ATPase H^+ pump is required for regeneration but not wound healing or tail development. The V-ATPase is specifically upregulated in existing wound cells by 6 hours post-amputation. Pharmacological or molecular genetic loss of V-ATPase function and the consequent strong depolarization abrogates regeneration without inducing apoptosis. Uncut tails are normally mostly polarized, with discrete populations of depolarized cells throughout. After amputation, the normal regeneration bud is depolarized, but by 24 hours post-amputation becomes rapidly repolarized by the activity of the V-ATPase, and an island of depolarized cells appears just anterior to the regeneration bud. Tail buds in a non-regenerative 'refractory' state instead remain highly depolarized relative to uncut or regenerating tails. Depolarization caused by V-ATPase loss-of-function results in a drastic reduction of cell proliferation in the bud, a profound mispatterning of neural components, and a failure to regenerate. Crucially, induction of H^+ flux is sufficient to rescue axonal patterning and tail outgrowth in otherwise non-regenerative conditions. These data provide the first detailed mechanistic synthesis of bioelectrical, molecular and cell-biological events underlying the regeneration of a complex vertebrate structure that includes spinal cord, and suggest a model of the biophysical and molecular steps underlying tail regeneration. Control of H^+ flows represents a very important new modality that, together with traditional biochemical approaches, may eventually allow augmentation of regeneration for therapeutic applications.

KEY WORDS: Regeneration, *Xenopus*, Tail, Ion pump, H^+ flow

INTRODUCTION

Extensive physiological data implicate endogenous ion flows in the control of regeneration and development (reviewed by Borgens et al., 1989; Levin, 2003; Nuccitelli, 1988; Robinson and Messerli, 2003). Imposition of currents on the order of 10 μA across severed spinal cords results in remarkable augmentation of regeneration in lamprey and guinea pig (Borgens et al., 1987; Borgens et al., 1990; Borgens et al., 1986). Applied electric fields are known to enhance limb regeneration in amphibia (Borgens et al., 1979; Borgens et al., 1977), and sciatic (Kerns and Lucchinetti, 1992; McDevitt et al., 1987) and optic nerve (Politis et al., 1988) repair in mammals. Indeed, these data have driven clinical trials in human subjects (Shapiro et al., 2005). However, the molecular sources of relevant currents and the downstream target mechanisms underlying the control of basic cellular functions by bioelectrical signals remain poorly understood. Without complete molecular characterization of the endogenous mechanisms underlying bioelectrical controls of growth and patterning (Levin et al., 2002; Zhao et al., 2006), the most precise and accurate approaches to control and correction of these signaling pathways will remain out of reach. Thus, to capitalize upon the considerable basic and biomedical potential of these novel cellular signals, it is necessary to understand the genetic components that underlie bioelectrical events during development and regeneration.

Center for Regenerative and Developmental Biology, Forsyth Institute, and Developmental Biology Department, Harvard School of Dental Medicine, 140 The Fenway, Boston, MA 02115, USA.

*Author for correspondence (e-mail: mlevin@forsyth.org)

Accepted 17 January 2007

The *Xenopus* tadpole regenerates its tail, restoring nerve, muscle, skin and blood vessel components (Deuchar, 1975). This robust and rapid ability to regenerate a complex appendage is a tractable model for the investigation of this biomedically important phenomenon (Gargioli and Slack, 2004; Ishino et al., 2003; Ryffel et al., 2003; Slack et al., 2004; Sugiura et al., 2004). Regeneration possesses a number of distinct phases (Abdel-Karim et al., 1990; Cadinouche et al., 1999; Gardiner et al., 2002). Shortly after amputation and wound healing, an initial swelling gives rise to a regeneration bud, in which proliferating cells rapidly rebuild the tail. This ability is stage-specific, and a non-permissive 'refractory' period has recently been identified [stage (st.) 45-47]; when larvae are amputated during this time, regeneration does not take place (Beck et al., 2003), although regeneration can be enabled during this period by activation of BMP or Notch pathways (Beck et al., 2003; Slack et al., 2004). In children, the ability to regenerate fingertips is lost at approximately 7 years of age (Douglas, 1972; Illingworth, 1974); thus, the refractory period represents an exciting opportunity to understand and learn to overcome endogenous time-dependent loss of regenerative ability.

The spinal cord, notochord and muscle all regenerate from the corresponding tissue in the stump (Slack et al., 2004), and metaplasia between differentiated cell types in the tail probably does not occur in frog embryos as it does in axolotl (making frog regeneration more similar to tissue renewal in mammals than to Urodele tail regeneration) (Gargioli and Slack, 2004). Here we use the term 'regeneration bud' instead of blastema, because it is not known whether all of the regenerating tissues in *Xenopus* can properly be called a blastema (Gargioli and Slack, 2004).

Because *Xenopus* has enabled molecular advances in regeneration biology (Cannata et al., 2001; Ishino et al., 2003; Slack et al., 2004; Tassava, 2004; Tazaki et al., 2005) and is ideal for investigations of

biophysical controls of pattern formation (Adams et al., 2006; Esser et al., 2006), we sought to gain mechanistic insight into the control of regeneration by ion flows in the *Xenopus* larval tail. Our physiological, genetic and cell-biological data show that H^+ flux (driven endogenously by the V-ATPase pump) underlies profound changes in membrane voltage, is necessary for initiating regeneration of the tail and correct neuronal patterning in the new tissue, and is sufficient to rescue both regeneration and axonal patterning in regeneration-refractory contexts. From these results, we synthesize a model of the molecular and biophysical events underlying tail regeneration.

MATERIALS AND METHODS

Amputation procedure and pharmacological regeneration screen

We performed a loss-of-function drug screen (Adams and Levin, 2006a; Adams and Levin, 2006b) that relies on the use of blocker reagents, proceeding from substances of low specificity to those with high specificity, guided by a hierarchical tree of ion-transporter inhibitors. This technique has uncovered transporters involved in morphogenetic events in both vertebrates and invertebrates (Duboc et al., 2005; Etter et al., 1999; Gasque et al., 2005; Hibino et al., 2006; Pyza et al., 2004; Shimeld and Levin, 2006).

For a list of compounds that were tested for their ability to specifically inhibit regeneration while permitting normal primary tail development, wound healing and general embryogenesis, see Table S1 in the supplementary material. Any target(s) of a reagent was ruled out for further consideration when a given compound did not affect regeneration, and in these cases broader specificity is a benefit because it allows a greater number of candidates to be filtered out. This screen implicated the V-ATPase transporter that we subsequently validated molecularly and characterized. However, the results of this screen do not prove that this is the only transporter that is important, and others may exist for which no blocker is yet available.

Xenopus laevis larval tails at st. 40-41 (Nieuwkoop and Faber, 1967) were amputated under a dissecting microscope using a scalpel blade at the point where the tail begins to taper. Amputated larvae were cultured in 0.1×Marc's Modified Ringer's (MMR) containing gentamycin, with and without the drug under test, at 22°C for 7 days and scored for regeneration as described below. Drug experiments (see Table S2 in the supplementary material) were repeated at least once, on a separate day using larvae from a different male/female pair, with each sample containing 50-100 larvae. Compounds (dissolved in 0.1×MMR) were applied at the dose indicated immediately after amputation. Because crowding may alter regenerative ability, larvae were cultured at a density of ~1 tadpole per ml (sufficient for normal growth and robust regeneration). Controls for effects of concanamycin on primary tail growth were performed by incubating embryos from st. 25 to 42, and assaying length and morphology of the tail for comparison with vehicle-only controls.

Palytoxin exposure

Palytoxin (PTX) is a protein from *Palythoa tuberculosa* that converts ubiquitous Na^+/K^+ transporters into a non-specific pore leading to rapid depolarization (Castle and Strichartz, 1988; Hilgemann, 2003; Tosteson et al., 1997; Tosteson et al., 2003), and thus is a useful reagent to probe the consequences of depolarization independent of downregulation of specific transporter expression. When exposed to 2 nM PTX for 5 days after amputation at st. 41, larvae were healthy and behaved normally, despite the inability to regenerate. This dose optimizes the trade-off between penetrance of the loss-of-regeneration phenotype and general toxicity.

Scoring of regeneration efficiency

To quantify and compare regeneration efficiency of larvae under different conditions, we introduced an ordinal measure: the 'Regeneration Index' (RI). Individual larvae within a Petri dish comprising a specific treatment, 5-7 days after amputation, were divided into the following categories:

++, complete regeneration (regenerated tail, indistinguishable from uncut controls);

+, robust regeneration with minor defects (missing fin, curved axis);

+/–, poor regeneration (hypomorphic regenerates); and

–, no regeneration.

The ratios of larvae in each category were calculated; percentages were then multiplied by 3, 2, 1 or 0 for ++, +, +/– or –, respectively. The RI for a dish ranged from 0-300, with the extreme values corresponding, respectively, to no regeneration and full regeneration in all larvae. The RI evaluates the efficiency of regeneration at the single-dish level and allows ready comparison of the effect of treatments with controls. This is a more sensitive metric than length because it takes into account both outgrowth and dorsoventral patterning.

Proliferating cell quantification

Fixed specimens at the stages indicated were processed for immunohistochemistry with H3P (phosphorylated Histone 3B) antibody. Bleaching of natural melanocyte pigments in samples allowed easy counting of H3P-positive cells in whole-mounts. Cells were counted manually in the triangular region of tissue present caudal to the amputation plane. Between four and six samples were counted for each stage and each condition. Sectioning revealed that reagent penetration and chromogenic staining were not confounding factors in H3P-positive cell detection (data not shown).

Confocal imaging of membrane voltage

Although electrophysiology provides a quantitative measure of membrane voltage, we chose voltage dyes because: (1) we sought a broad spatial characterization of voltage gradients in the tail and bud; (2) we wanted to observe the system in a less invasive way (puncturing epithelia often gives rise to confounding injury currents); and (3) in this system, traditional electrode techniques do not easily allow one to distinguish between transepithelial potential and transmembrane gradients.

Because $DiBAC_4(3)$ (hereafter DiBAC) is anionic, the more depolarized a cell, the greater the accumulation of the permeant dye and the greater the intensity of intracellular, relative to extracellular, fluorescence. Successful absolute mV calibration of this dye has not yet been accomplished in this system because of the difficulties in simultaneously controlling $[H^+]$ and $[K^+]$, and of performing electrophysiology in single cells in the tail. Therefore, many controls (see Figs S1, S2 and S3 in the supplementary material) were performed [including autofluorescence spectra, high-magnification examination of signal homogeneity within individual cells, predicted changes in signal when cells were artificially depolarized by ionophores and manipulation of extracellular ion content, imaging with the complementary cationic dye $DiSBAC_4(2)$]. Our analysis of the DiBAC data is very conservative. Briefly, depolarization of cells with ionophores led to the expected increase in DiBAC fluorescence and, observations using $DiSBAC_4(2)$, a cationic dye whose fluorescence decreases in response to depolarization, gave the same result as DiBAC. To maximize the information content, the conditions of imaging, including laser intensity and photomultiplier gain (or exposure time), were kept as constant as possible. Photoshop (Adobe) was used to describe the results quantitatively.

Patterns of DiBAC fluorescence were characterized (Fig. 3E) as follows: 'Maximum' projections of *z*-series through stained tails were made on one of the confocal microscopes. Maximum, which displays the brightest pixel from each column of the stack to create a single image summary, was chosen because tails do not lie flat on the slide and their cross-section is not consistent; the other available projection algorithms would, therefore, each be accounting for the contribution of pixels that in fact represent the intensity of fluorescence outside the tissue. Projections were saved using the Red-Green-Blue color look-up table; this uses color, rather than brightness, to distinguish among different pixel intensities, with red being brightest (most depolarized) and blue dimmest (most polarized). Using Photoshop, identical circular ROIs (regions of interest) were drawn on the projection: the first centered in the bud, as far posterior as possible; the second centered in the shoulder region; the third placed posterior to the shoulder, over undisturbed somites (see Fig. 3E; records of these ROIs are available on request, and examples are shown in Fig. 3 and see Fig. S3 in the supplementary material). The first ROI was placed, then the 'select color range' function was used to count the number of pixels within the ROI that fall in the intensity range represented by red, green and blue pixels, and to determine their mean intensity. The second ROI was then drawn and the process was repeated.

Finally, pixels in the third ROI were measured and counted. Using these colors insured that no saturated or underexposed pixels would be included in the quantification. Each mean intensity was multiplied by the number of pixels at that intensity, and those products were summed to give a total intensity for each ROI on each tail. The mean total intensity for each ROI in each region was then calculated, and normalized to the mean total intensity of the undisturbed cells of the regenerating tail. The points on the graph shown in Fig. 3E therefore show a measure of the center of the data. It is important to note, however, that there was sometimes large variation among individuals in the same sample. The graph and the images shown illustrate the most commonly seen pattern. Fluorescence images shown in Fig. 3 were not manipulated except to crop and resize in preparation of the figure.

Xenopus larvae were soaked in the voltage-sensitive dye DiBAC or DiSBAC (Invitrogen), at a final concentration of 10 ng/ml in 0.1×MMR in the dark for at least 30 minutes, then imaged with a Leica TCS SP2 Confocal Imaging system, mounted on a Leica upright DM RXE microscope. The dye was excited at 488 nm and a 20 nm band of emission wavelengths centered at 515 nm was collected. Alternatively, images were produced using an Olympus spinning disc confocal (FITC filter) mounted on an Olympus BX61 compound microscope. Data were collected using a Hamamatsu Orca AG CCD camera. Representative images shown in Fig. 3 were chosen on the basis of their brightness and fluorescence distribution falling in the middle of the range of intensities for that treatment, as determined by eye.

γ-Irradiation

Intact larvae were subjected to 10^4 rads of gamma-irradiation in a Cs^{137} irradiator. Larvae were then split into subgroups, one of which underwent amputation 24 hours after the irradiation procedure. Larvae were fixed at 24 hpa or 5 dpa for immunohistochemistry.

Ion transporter misexpression

Approximately 5 ng of each construct mRNA (transcribed in vitro from YCHE78, PMA1.2 and PMA248 plasmids) was mixed with 50 ng of rhodamine-labeled dextran and 250 pg of mRNA encoding β-galactosidase, RFP or GFP (Zernicka-Goetz et al., 1996) (as lineage labels) and injected into the 1- or 2-cell stage embryo. These mRNAs are still strongly expressed at the time of amputation [e.g. Fig. 1F′,F″ for PMA expression persisting at st. 47; and for label protein persisting to st. 46 (Levin and Mercola, 1998)]. By using co-injection of a fluorescent lineage label and later selecting embryos with the desired localization (using a dissecting scope with epifluorescence) prior to amputation, we were able to analyze larvae expressing a desired construct in various anatomical regions.

Statistical analysis

To compare among three or more treatments, raw data (not RIs) from the regeneration efficiency scoring were analyzed using a Kruskal-Wallis test for ordinal data, with H corrected for tied ranks. Post-hoc comparisons were made using Dunn's Q. To compare between two treatments, data were analyzed using a Mann-Whitney *U* test for ordinal data with tied ranks, using a normal approximation for large sample sizes. Flank cell data were analyzed using a two-factorial (age, treatment) ANOVA. For complete statistical results, see Table S2 in the supplementary material. Differences were considered significant if $P<0.01$.

Western blotting

Twenty-five *Xenopus* larvae at st. 40 were resuspended in lysis buffer (1% Triton X-100, 50 mM NaCl, 10 mM NaF, 1 mM Na_3VO_4, 5 mM EDTA, 10 mM Tris pH 7.6, 2 mM PMSF). Protein solution was mixed at 1:1 with Laemmli sample buffer (Bio-Rad) containing 2.5% 2-mercaptoethanol. The proteins were fractionated by SDS-PAGE and electrotransferred to a PVDF membrane. After washing, the membrane was blocked with 3% bovine serum albumin and 5% dry milk in Tris-buffered saline including 0.1% Tween 20. The membrane was then incubated overnight in a Mini-PROTEAN II multiscreen apparatus (Bio-Rad) at 4°C with the primary antibody diluted 1:2000 in TTBS plus 3% BSA and 5% dry milk. After washing, the blots were incubated with peroxidase-conjugated secondary antibody (1:5000) and developed using the ImmunoStar Chemiluminescent Protein Detection System (Bio-Rad).

In situ hybridization

Larvae were fixed in MEMFA (Sive et al., 2000) and dehydrated in methanol, followed by in situ hybridization according to standard protocols (Harland, 1991). Ion-transporter constructs used to generate probes were KCNK1 (BC042262, Open Biosystems) and V-ATPase 16 kD subunit (BE025959, RZPD). Experiments included sense probe controls which, as expected, exhibited no signal (data not shown).

Immunohistochemistry

Xenopus larvae were fixed overnight in MEMFA, heated for 2 hours at 65°C in 50% formamide (this was not done when using fluorescent secondary antibodies), permeabilized in PBS plus 0.1% Tween 20 and 0.1% Triton X-100 for 30 minutes, and processed for immunohistochemistry using alkaline phosphatase-conjugated secondary antibody as described previously (Levin, 2004) until signal was optimal and background was minimal (usually 12 hours). Anti-ductin (V-ATPase c subunit) antibody, generated against peptide DAGVRGTAQQPR by Invitrogen, reveals one single clear band of predicted size on a western blot and was used at 1:500. Anti-Caspase-3 (Abcam #AB13847), anti-acetylated α-tubulin (Sigma #T6793), and anti-phosphorylated histone H3B (Upstate #05-598) were used at 1:1000. Anti-KCNK1 [a generous gift of S. A. Goldstein (University of Chicago, IL) and D. Bockenhauer (Yale University, CT)] was used at 1:500. Anti-PMA1 (Santa Cruz Biotechnology SC-33735) was used at 1:200.

Axon detection was performed using AlexaFluor 555-conjugated goat anti-mouse secondary antibody (Invitrogen) at 1:500. Fluorescence images were collected on a Leica TCS SP2 confocal imaging system at λ_{ex}=543 or an Olympus BX61 with the TRITC cube. Some larvae were embedded in JB4 (Polysciences) and sectioned at 30 μm. Control experiments omitting primary or secondary antibody showed no signal (data not shown). Images in Fig. 1G′ and Fig. 5A-G were processed using Adobe Photoshop as follows. Background autofluorescence was removed by segmentation of the original fluorescence images. The brightest pixels could readily be selected such that the selection best represented the pattern of axons. This selection was then pasted onto the transmitted light photographs of the same sample. The original unmanipulated images are available on request. Overall image brightness was adjusted for optimal clarity. Images and localization data presented in all expression figures represent consensus patterns obtained from analysis of at least 15 larvae in all experiments.

RESULTS

V-ATPase activity in the tail is required for regeneration

We performed a loss-of-function pharmacological screen (Adams and Levin, 2006a; Adams and Levin, 2006c) in *Xenopus* larvae designed to identify endogenous ion transporters that are required for tail regeneration but not involved in general embryogenesis, wound healing or primary tail development (see Table S1 in the supplementary material). The assay quantified regeneration efficiency using a 'regeneration index' (RI), which uses a scale from 0 to 300, with 300 representing complete regeneration.

Normal regeneration resulted when larvae amputated at st. 41 (Fig. 1A,A′) were exposed to a wide variety of pharmacological reagents (see Table S1 in the supplementary material). By contrast, exposure to 150 nM concanamycin, a potent and highly specific inhibitor of the V-ATPase H^+ pump (Huss et al., 2002), resulted in a strong inhibition of regeneration (Fig. 1B,B′) in the absence of general toxicity or developmental abnormalities (RI reduced from 216 to 49, n=226, $P \ll 0.001$) (see Table S2 in the supplementary material). Therefore, we focused on the V-ATPase (Nishi, 2002), which generates voltage gradients at the expense of ATP, when expressed in vesicular or cell plasma membranes (Wieczorek et al., 1999). Analysis of the localization of activated Caspase-3 in control and V-ATPase-inhibited larvae (Fig. 1C,D) revealed that regenerating tails normally possess a small apoptotic cell group (Tseng et al., 2007), but no increase in the degree of apoptosis was

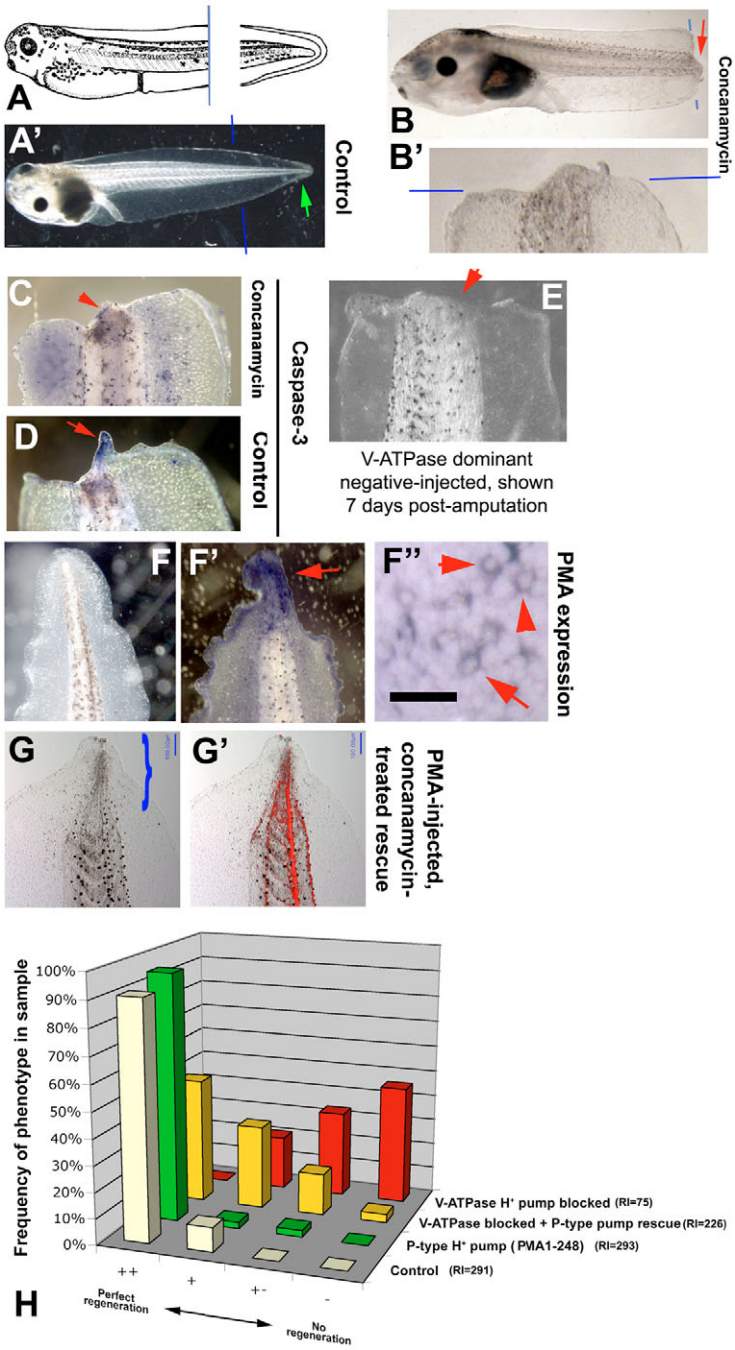

Fig. 1. The V-ATPase is required for tail regeneration in *Xenopus*. When amputated at st. 41 (**A**), the *Xenopus laevis* larva (n>1000) rapidly rebuilds a tail (**A'**). Regeneration, but not anterior development, primary tail growth or wound healing, is abolished by specific inhibition of the V-ATPase H^+ pump (n=226) by concanamycin treatment immediately after cutting (**B**; close-up shown in **B'**). Blue lines in A-B′ indicate approximate amputation plane. This inhibition of regeneration is not due to an upregulation of apoptosis, as concanamycin-treated tails (**C**) do not show a greater degree of staining for the apoptosis marker activated Caspase-3 than controls (**D**) when processed at 48 hpa. When the dominant-negative V-ATPase E subunit is expressed in tails, regeneration is not observed (**E**, compare with B′, n=66), while otherwise normal development continues. For statistical analyses, see Table S2 in the supplementary material. (**F-H**) We attempted to rescue the V-ATPase-inhibited phenotype with misexpression of a single-subunit concanamycin-insensitive H^+ pump, PMA. (F-F″) Immunohistochemistry with antibody to PMA. Larvae were microinjected with PMA construct+GFP at the 1-cell stage, and sorted at tailbud or later stages for GFP expression in the tail. (F) Negative control larva injected with β-gal and probed with PMA antibody, showing no signal. (F′) Positive staining in regeneration bud confirms that injected constructs lead to robust levels of expression in the tail during regeneration when mRNA is injected at 1-cell stage. (F″) Close-up of PMA-expressing cells demonstrating the predicted cell-membrane localization of H^+ pump (red arrows). Scale bar: 50 μm in panel F″. (G,G′) Such expression of the PMA pump is sufficient to rescue regeneration after V-ATPase inhibition by concanamycin. (G) Tails of larvae injected with PMA at the 1-cell stage, amputated at st. 41, and then incubated in concanamycin regenerate (compare with phenotype in B′). Newly regenerated tissue is indicated by the blue bracket. (G′) Normal neuronal pattern revealed by immunohistochemistry. (H) Quantification of rescue effect. Abrogation of regeneration (red bars) can be largely prevented by misexpression of PMA (dark yellow bars, n=127), demonstrating the necessity for the H^+ flux during regeneration (off-white bars, no treatment; green bars, PMA injection only).

observed after V-ATPase inhibition, suggesting that an upregulation of cell death does not account for this failure to regenerate and is not a consequence of V-ATPase inhibition (as might be expected if growth was stunted owing to abrogation of an essential housekeeping function).

Injections of mRNA into the 1-cell, fertilized *Xenopus* egg result in mosaic expression (Sive et al., 2000). We took advantage of this to explore the spatial properties of the V-ATPase activity, as early injections result in a population of embryos exhibiting varied (random) localizations of exogenous protein that can be later sorted into subgroups according to the different areas that have been reached. By co-injecting a fluorescent lineage label and selecting embryos with the desired localization (using a dissecting scope with epifluorescence) prior to amputation, we were able to analyze embryos expressing a desired construct in head, tail, etc. (a posteriori sorting). Moreover, mRNAs injected in this manner can produce protein that is still robustly expressed at the time of amputation [e.g. ion pump mRNA shown in Fig. 1F′,F″, and marker mRNA shown by Levin and Mercola (Levin and Mercola, 1998)]. We utilized this technique rather than targeted electroporation into the tail region because the process of electroporation itself appeared to non-specifically interfere with the subsequent ability to regenerate (data not shown).

To confirm the role of V-ATPase in regeneration, we phenocopied the pharmacological phenotype by misexpression of mRNA encoding a molecular loss-of-function construct. We chose to use a protein-specific dominant-negative approach rather than morpholinos because the frog embryo contains considerable

amounts of maternal V-ATPase protein (Adams et al., 2006) that would remain untouched by techniques targeting mRNA. Using a well-characterized dominant-negative V-ATPase E subunit, YCHE78, that specifically abrogates the activity of the V-ATPase complex (Lu et al., 2002), we observed the same phenotype as that obtained with concanamycin: YCHE78 misexpression in the tail prevented regeneration when cut at st. 41 (Fig. 1E) as compared with injected animals not exhibiting YCHE78 expression in the tail (n=66, P<0.01) (see Table S2 in the supplementary material). These data strongly support the necessity for endogenous local V-ATPase function in the tail for regeneration.

The crucial activity for regeneration is cell-surface H^+ pumping

To test whether it is the H^+ pumping activity of the V-ATPase that is important for regeneration, we misexpressed a concanamycin-insensitive yeast P-type H^+ pump, PMA (Masuda and Montero-Lomeli, 2000). Control larvae (injected with β-gal mRNA) exhibited no signal in immunohistochemistry with an anti-PMA antibody (Fig. 1F). By contrast, larvae from embryos injected with PMA mRNA often exhibited strong expression in the regenerating tissue (Fig. 1F′,F″). Misexpression of PMA in the tail largely prevented the strong inhibition of regeneration by pharmacological V-ATPase blockade [Fig. 1G,G′,H; embryos scored 7 days post-amputation (dpa); there was a 3-fold increase in RI relative to concanamycin-exposed embryos; n=127, P<0.01 (see Table S2 in the supplementary material)]. This rescue experiment demonstrated that it is indeed H^+ pumping endogenously provided by the V-ATPase that is blocked by concanamycin, and that this normally ensures complete regeneration, ruling out possible cryptic functions of the V-ATPase complex in regeneration. Crucially, because PMA is a cell-surface H^+ pump only (Bowman et al., 1997) (Fig. 1F″), its ability to rescue the concanamycin phenotype demonstrates that it is the plasma membrane, not the vesicle membrane functions of the V-ATPase that are important for regeneration.

Cell-surface expression of V-ATPase is rapidly induced in existing cells

We next examined endogenous expression of V-ATPase in the regeneration bud of larvae cut at st. 41. Most ion translocators are absent from the regeneration bud (Fig. 2A,A′). By contrast, the c subunit of the V-ATPase was expressed at the mRNA (Fig. 2B,B′) and protein (Fig. 2C,C′) levels, specifically in the regeneration bud, within 6 hours post-amputation (hpa). A low level of background expression elsewhere in the trunk was detected, owing to the ubiquity of vesicular V-ATPase (DNS). Strong plasma membrane expression (Fig. 2C″) was observed in the regeneration bud, in cells of the epithelium covering the bud, and in mesenchyme cells immediately under the wound epithelium (see also Fig. S4 in the supplementary material, which shows a later time-course). Consistently, preliminary observations indicated a strong H^+ efflux from the surface of bud cells at 24 hpa, as measured using an

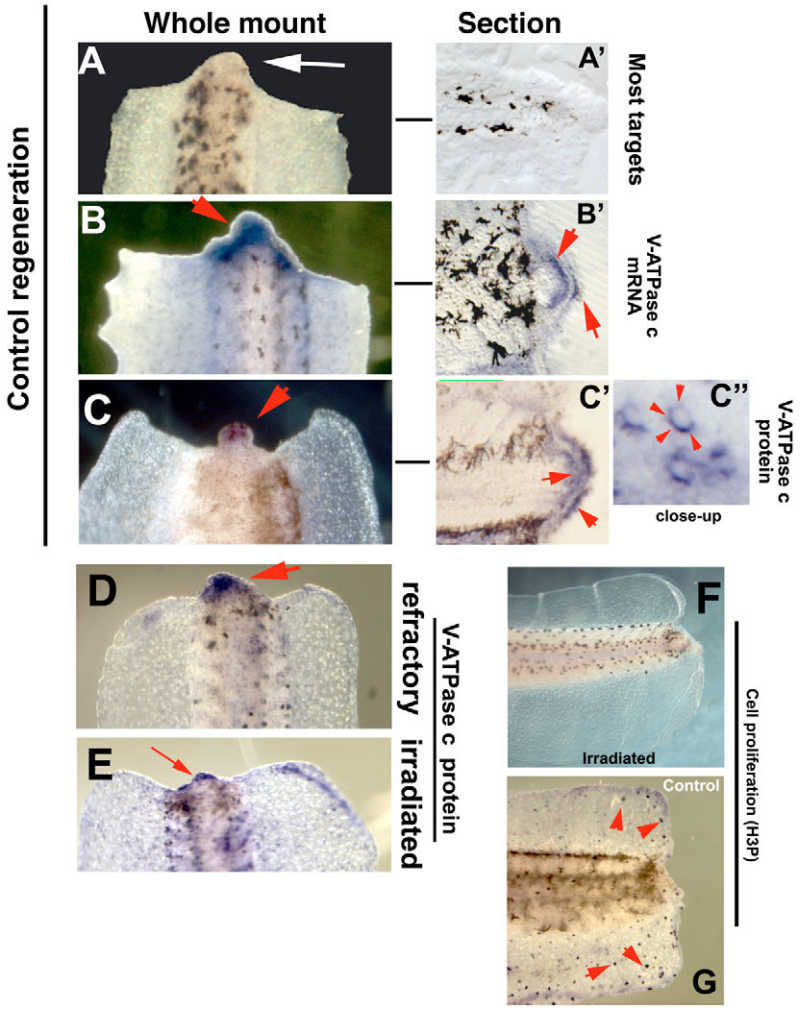

Fig. 2. Characterization of V-ATPase expression and physiology. Whereas NaV1.5 (**A**,**A′**) and most transporter genes tested, including Kir6.2 and subunits of the H^+/K^+-ATPase, are absent, both V-ATPase mRNA and protein are detected in the regeneration bud (**B**,**B′**,**C**,**C′**). High magnification of section reveals the predicted cell-membrane localization for the protein (**C″**; scale similar to Fig. 1F″). (**D**) As in regenerating tails, amputation during the refractory period (st. 46) results in V-ATPase protein expression at 24 hpa. The same is true in irradiated larvae examined at 48 hpa (**E**), which exhibit no cell proliferation, as detected by the phosphorylated Histone H3B marker (**F**, compare with normal pattern of proliferation in **G**). Sections were generated as described by Levin (Levin, 2004). Larvae shown in A-E are oriented with anterior towards the bottom; sections A′,B′,C′,F′,G′ are oriented with anterior to the right and dorsal upwards. Larvae in F,G are shown at 48 hpa. White arrowhead points to regeneration bud with lack of expression. Red arrows and arrowheads indicate positive signal (expression of RNA or protein marker).

extracellular, self-referencing ion-selective (SERIS) probe (K. R. Robinson and D.S.A., personal communication). Thus, the pump is expressed in a spatio-temporal pattern consistent with an endogenous role in the regeneration bud; moreover, the cell-surface expression is consistent with the observed rescue of regeneration by a H^+ pump that is only functional in the plasma membrane, not vesicles (Fig. 1F″).

We also investigated tails cut during the 'refractory' period. V-ATPase expression was observed in tails cut at st. 46-47 and fixed at 24 hpa (Fig. 2D), suggesting that their inability to regenerate was not due to the failure to induce V-ATPase expression in the regeneration bud, but rather to a problem with a physiological process downstream of V-ATPase-component translation.

To determine whether the V-ATPase is normally upregulated in existing cells or produced by a new cell population generated in response to amputation, we irradiated larvae, a procedure that abolishes cell proliferation (Li et al., 2001; Salo and Baguna, 1985). Irradiated larvae still upregulated V-ATPase expression in the wound (Fig. 2E), despite confirmed loss of proliferative cells (Fig. 2F,G), suggesting that the V-ATPase upregulation takes place in existing wound cells and does not require the production of a new cell type in the regeneration bud.

V-ATPase regulates membrane voltage in regeneration bud cells

We next directly examined the physiology of the regeneration bud using the voltage-reporter dye bis-(1,3-dibutylbarbituric acid)pentamethine oxonol ($DiBAC_4(3)$; referred to here as DiBAC) (Epps et al., 1994), after confirming, using ionophores and high $[H^+]$ and $[K^+]$ media, that in *Xenopus* tail cells measurable changes in fluorescence intensity of DiBAC are proportional to depolarization state (see Materials and methods and see Figs S1 and S2 in the supplementary material). The uncut, st. 41, regeneration-competent tail contained scattered populations of cells depolarized relative to the rest of the tail (Fig. 3A,A′). At 6 hpa in a regenerating tail, cells of the bud were depolarized relative to the rest of the tail (Fig. 3C,E). Then, consistent with the above data implicating control of ion flow in the bud by the V-ATPase (a hyperpolarizing transporter) upregulated during the first 6-12 hpa, we found that by 24 hpa, the cells of the bud had largely repolarized (Fig. 3D). Staining with the cationic oxonol $DiSBAC_4(2)$, a slow-response membrane voltage probe, confirmed that the bud was repolarized (see Fig. S3 in the supplementary material). Interestingly, by 24 hpa, a new domain of depolarized cells appeared in what we term the 'shoulder' region (Fig. 3B,D,E). As expected, tails treated with the V-ATPase-inhibitor concanamycin showed strong depolarization in the bud and throughout the tail (Fig. 3F,F′), and refractory tails (Fig. 3G-G″,E) failed to repolarize the regeneration buds by 24 hpa, unlike regeneration-competent larvae.

To ask whether an effect on membrane voltage is a mechanism by which the V-ATPase pump controls regeneration, we depolarized tails without directly targeting V-ATPase, using 2 nM PTX, which converts the Na^+/K^+-ATPase into a Na^+/K^+ channel (Castle and Strichartz, 1988; Hilgemann, 2003). This resulted in a 33% reduction in the RI (n=81, P=0.002) despite normal health and behavior, demonstrating that the regeneration bud is more dependent on membrane voltage level than cells elsewhere, and suggesting that the membrane voltage (and downstream voltage-sensitive pathways) is indeed relevant for regeneration. Based on these DiBAC and functional data we conclude that, consistent with its expression and the known functions of the V-ATPase throughout phyla (Wieczorek et al., 1999), the ion pumping activity of the V-ATPase is an important determinant of the steady-state membrane polarization level in the regeneration bud cells, and that the membrane voltage range differs in predictable ways in regeneration-competent and regeneration-incompetent tails.

H^+ pumping rescues regeneration of refractory tails

To determine whether induction of H^+ flow is a promising strategy for inducing regeneration, we attempted to rescue regenerative ability during the refractory period by misexpression of the yeast PMA H^+ pump, which would tend to repolarize the bud (mimicking the function of the V-ATPase). Expression of PMA exhibited the predicted cell-membrane localization pattern (Fig. 1F′,F″). Remarkably, expression of PMA led to regeneration in a significant number of refractory tails (Fig. 3I-I″,K). More than twice as many injected tails regenerated to some degree (36% compared with 15% of controls), and of those that regenerated, PMA-injected embryos regenerated to a much better degree (compare Fig. 3H″ with I″; Fig. 3K), with 18% of injected embryos showing good or perfect regeneration as compared with 5% of controls. A Mann-Whitney U test to compare degrees of regeneration confirmed that this difference is highly significant (n=103, $P \ll 0.001$).

To confirm that PMA rescue was related to membrane potential changes, DiBAC was used to visualize PMA-rescued tails for comparison with refractory tails. We found that PMA-injected embryos that subsequently went on to regenerate (Fig. 3J,J′) had indeed repolarized their buds relative to unmanipulated refractory tails (compare Fig. 3J with 3G′) and, as predicted, had the characteristic relative-depolarization of the shoulder (Fig. 3E). The ability of a heterologous H^+ pump to repolarize the bud and induce regeneration suggests that PMA is not susceptible to the post-translational events that inhibit V-ATPase in refractory tails, and confirms that PMA may be a useful reagent for rational modulation of bioelectric conditions in vivo.

V-ATPase controls cell proliferation in the bud

Failure to regenerate after V-ATPase inhibition could be due to insufficient cell growth and/or a lack of morphogenetic cues. To gain insight into cellular mechanisms through which the V-ATPase controls outgrowth (to link V-ATPase activity to downstream effector modules), we characterized cell proliferation using an antibody to phosphorylated Histone H3B, which is a standard marker of cells in the G2-M transition of the cell cycle, and useful for identifying mitotic cells in regenerating systems including *Xenopus* (Saka and Smith, 2001; Sanchez Alvarado, 2003). At 24 hpa, this subset of proliferating cells was found to be homogenously distributed throughout the growing tail (Fig. 4A). By 48 hpa, these cells were highly enriched in the regeneration bud, but often largely absent from the region of the flank anterior to the amputation (Fig. 4B). Specific inhibition of the V-ATPase resulted in an ~6-fold decrease in the number of proliferating cells in the bud (Fig. 4C-D′), but only a 2.5-fold decrease in the number of proliferating cells in the flank at 24 hpa (this reduction did not noticeably impair larval development or behavior). These data reveal that the V-ATPase is required for the upregulation of proliferation in the growth zone by 48 hpa, demonstrating that the effect of this pump is distinct in the regeneration zone from that in other tissues. The normal development of uncut embryos cultured in concanamycin from fertilization (A.M., D.S.A. and M.L., unpublished) suggests that the contribution of the V-ATPase is much greater for regeneration than it is for normal growth.

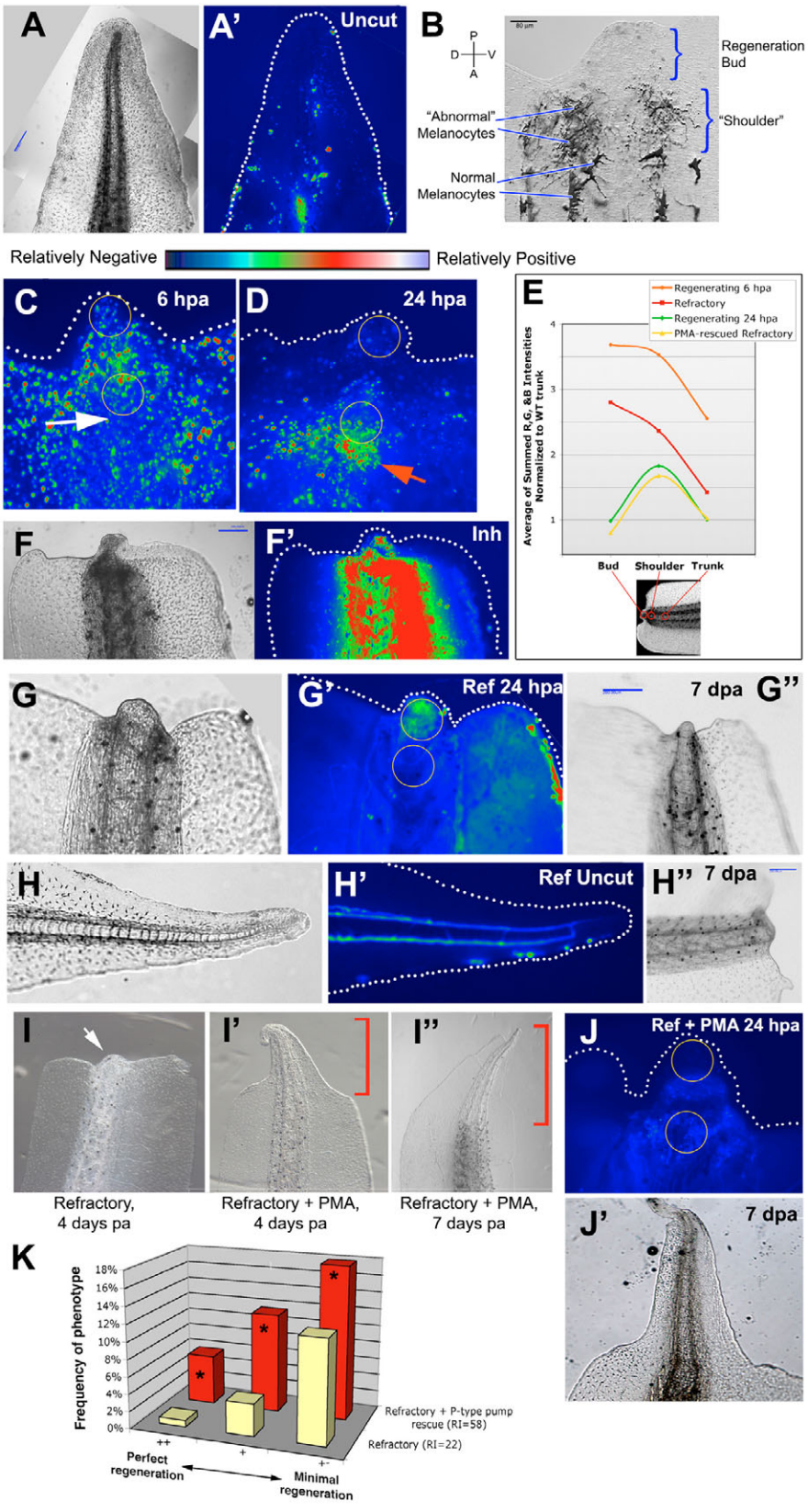

Fig. 3. Imaging of membrane voltage using DiBAC. Red indicates more depolarized than green, which is more depolarized than blue (see key under A′). For further description of the collection and analysis of the DiBAC data see Figs S1, S2 and S3 in the supplementary material. (**A**,**A′**) An uncut tail from a st. 41-43 larva shows generally even voltage levels (blue areas), with scattered cells (green to red) that are depolarized relative to the rest of the tail. Scale bar: 250 μm. (**B**) Transmitted light image of a regenerating tail bud with the different regions labeled. The shoulder is defined as the region underlying the abnormally shaped melanocytes; this region appears darker in lower magnification images (e.g. F). Scale bar: 80 μm. (**C**) Regenerating tail bud imaged at 6 hpa. At this early time point, the bud is depolarized relative to the surrounding tissue. Yellow circles indicate bud and shoulder regions of interest (ROIs) that were used in quantifying this image (trunk ROI not shown on these cropped images). (**D**) Tail imaged at 24 hpa. The bud has repolarized relative to the 6 hpa state. The appearance of DiBAC fluorescence is similar to that in uncut tails, with the exception of the shoulder region that has an island of depolarization. Although not visible in every tail, this was a very common pattern. Yellow circles indicate ROIs; arrow indicates the depolarized region of shoulder cells. (**E**) Comparison of the relative voltage patterns found in regenerating 24 hpa (green), regenerating 6 hpa (orange), refractory (red) and PMA-rescued refractory (yellow) tails. Both regenerating 24 hpa and PMA-rescued refractory tails are depolarized in the shoulder region relative to the bud and trunk. By contrast, refractory and 6 hpa tails are highly depolarized in the bud, becoming more polarized in anterior regions. (**F**,**F′**) Tail cut at st. 41 and treated with concanamycin. The large region of red and green indicates relatively strong depolarization, as predicted (V-ATPase polarizes, therefore the inhibitor should cause depolarization). (**G**,**G′**) At 24 hpa, the buds of refractory tails are depolarized relative to a regenerating tail. Yellow circles indicate ROIs. (**G″**) The same tail shown in G and G′ confirming that refractory tails fail to regenerate, even at 7 dpa. Scale bar: 250 μm. (**H**,**H′**) Uncut st. 46-47 (refractory) tail. DiBAC images of refractory tails vary; in this image, dorsal and ventral blood vessels are obvious. The most consistent difference between refractory and regeneration-competent tails is the relatively even staining across the refractory tail (compare with the 'spottiness' of staining in A′ and D). (**H″**) The same tail as H and H′ shown at 7 dpa, confirming that this tail was refractory when it was amputated. Scale bar: 250 μm. (**I**) Refractory tail shown 4 dpa. (**I′**) P-type pump-expressing tail, 4 dpa at the refractory stage. (**I″**) P-type pump-expressing tail, 7 dpa at the refractory stage, showing full regeneration. Red bracket indicates newly regenerated tissue absent in control tails. (**J**) DiBAC reveals that, unlike control refractory tails (G′), the bud of PMA-expressing refractory tails is relatively polarized, as with tails cut at st. 41 (D). Yellow circles indicate ROIs. (**J′**) The same tail as J, showing significant regeneration at 7 dpa. (**K**) Analysis of the rescue of regeneration in refractory tails by misexpression of a yeast P-type H^+ pump. Off-white bars, refractory tails; red bars, PMA-injected tails. Injection of PMA caused a significant augmentation of the ability of refractory tails to regenerate. *, indicates significantly different from controls (see Table S2 in the supplementary material).

V-ATPase function controls expression of early genes in the bud

We next sought to uncover functional links between V-ATPase activity and gene expression in the regeneration bud. Markers such as Notch (Slack et al., 2004) are only expressed later, and in tissue that does not exist in V-ATPase-inhibited larvae. Thus, we utilized immunohistochemistry with an earlier marker normally expressed by 12 hpa: the K^+ channel KCNK1 (Fig. 4E,E′). When V-ATPase activity was abrogated by concanamycin or by a 24-hour incubation in medium containing function-blocking anti-V-ATPase antibody, KCNK1 expression was absent (n=13, Fig. 4F-G′). Thus, V-ATPase is upstream of at least some gene expression in the regeneration bud, including that of other ion transporters specifically expressed during early stages of regeneration. (Here, KCNK1 was used only as a novel marker for early stages of regeneration in the *Xenopus* tail; evidence that KCNK1 may be functionally involved in regeneration will be presented elsewhere.)

V-ATPase-dependent H^+ flux controls axon pattern during regeneration

To characterize morphogenetic consequences of V-ATPase abrogation, we examined axons using an anti-acetylated α-tubulin antibody. In normally regenerating tails, axons appear to be increased in number relative to the uncut tail portion, and they extend into the bud in bundles parallel to the anterior-posterior axis (Fig. 5A). By contrast, axons of V-ATPase-inhibited tails increase in density, but axon patterning is abnormal, with axons absent from the middle of the regeneration bud (Fig. 5B) or appearing tangled at the tail tip (Fig. 5B′). These data demonstrate that V-ATPase is required not only for expression of marker genes in the regeneration bud and the increase in proliferation in the growth zone, but also for the patterning of axons in the tail. Consistently, our data show that expression of the yeast proton pump, which was able to rescue V-ATPase-inhibited and refractory-inhibited regeneration, also restored normal axon patterning to concanamycin-treated tails (Fig. 5C). Moreover, in normal refractory tails, there is no apparent increase in the number of axons, and those that are present terminate well anterior of the tail tip (Fig. 5D). However, expression of the yeast proton pump in refractory tails induced the proliferation and the axonal patterning normal to regeneration, both in tails that were rescued and in those in which regeneration was not induced (Fig. 5E,E′). In those larvae in which normal tail outgrowth was not rescued by PMA, the presence of axons at the very edge of the wound was induced in 25 of 30 animals (Fig. 5E), demonstrating that neural patterning and outgrowth are separate from the morphological regenerative response, with both downstream of H^+ flux.

Finally, to determine whether the abnormal axonal patterning observed in V-ATPase-inhibited larvae is caused by the inhibition of cell proliferation, we γ-irradiated larvae before amputation at st. 41 to abolish cell proliferation (Fig. 2F). In such animals, despite a lack of regeneration, axons extended all the way to the tip in bundles parallel to the main axis of the bud (Fig. 5F,G), in contrast to the situation after V-ATPase inhibition (Fig. 5B,B′). Thus, the patterning of axons depends upon V-ATPase activity in a pathway parallel to the induction of cell proliferation, and is not a secondary consequence of mitotic activity.

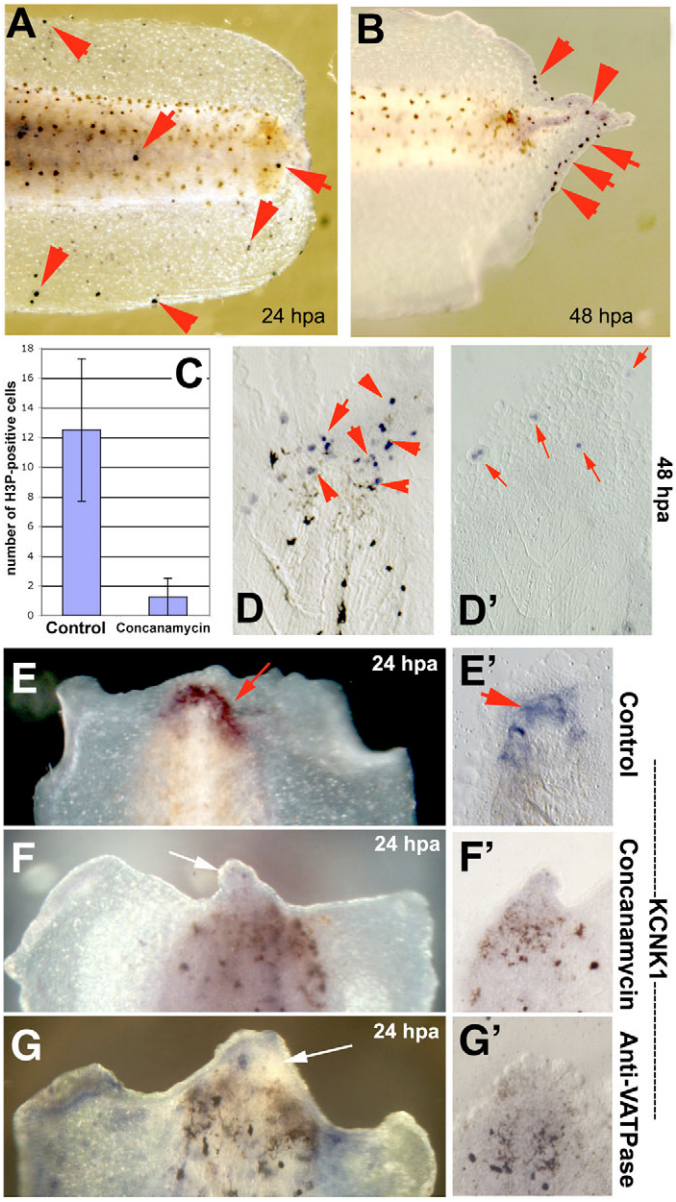

Fig. 4. V-ATPase function is required for the upregulation of cell proliferation in the tail regeneration bud. Proliferating cells were labeled with immunohistochemical staining for phosphorylated Histone H3B (H3-P). (**A**) At 24 hpa, proliferating cells in the G2-M transition are randomly distributed. (**B**) By 48 hpa, the proliferating cells cluster in the regeneration bud and have largely disappeared from the caudal flank. Red arrows indicate H3P-positive cells. (**C**) Incubation in concanamycin immediately after amputation reduces proliferation in the bud; sample proliferation data are from **D** (control) and **D′** (concanamycin-treated) larva. A,B are oriented anterior to the left; all other panels are oriented anterior upwards. n=8 for each condition. (**E-G′**) KCNK1 expression requires V-ATPase activity. The regeneration bud normally expresses the KCNK1 channel by 24 hpa (E,E′). By contrast, larvae in which the V-ATPase was inhibited by concanamycin (F,F′) or anti-c subunit antibody (G,G′) exhibit no KCNK1 expression at 24 hpa. n=10 for each condition. White arrows indicate lack of expression; red arrows indicate positive signal (expression of KCNK1).

DISCUSSION

Pursuing a complementary biophysical and genetic understanding of regeneration, we asked whether endogenous ion flows are involved in tail regeneration, what genetic elements underlie such currents, and what downstream cell behaviors are controlled by them. The characterization of early biophysical and molecular events revealed a number of novel and important aspects of regeneration biology.

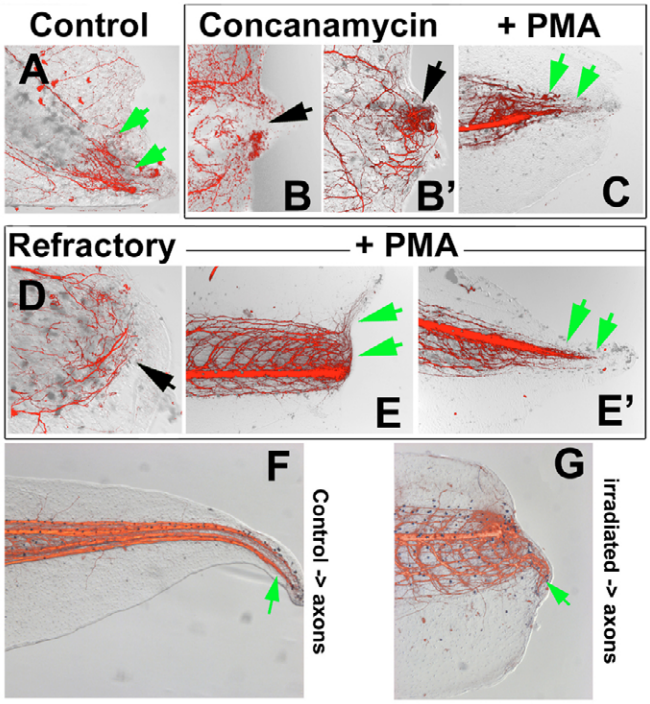

Fig. 5. Axonal growth pattern is dependent on H^+ fluxes. Green arrows indicate normal axon patterning; black arrows indicate abnormal axon number and/or location. (**A**) The normal pattern of regenerating axons is parallel to the main body axis, extending to the tip of the bud at 72 hpa. This is altered in V-ATPase-inhibited tails, where axons are absent from the central core of the new tissue of partial regenerates at 72 hpa (**B**), or are present in a tangled mass and not aligned parallel to the tail's primary axis (**B'**). The expression of the concanamycin-insensitive yeast PMA H^+ pump in the tail can rescue the normal axonal patterning (**C**). (**D**) In refractory-stage larvae, axons terminate in a loop at a considerable distance from the edge, and perpendicular to the main tail axis. Expression of PMA rescues the neuronal phenotype, resulting in axon growth to the very edge of the wound in non-regenerating tails (**E**), and parallel outgrowth of axons into the new tissue of regenerates (**E'**). The normal pattern of axons, reaching to the end of the tissue at 7 dpa (**F**), is not affected by irradiation (**G**), which abolishes cell proliferation and regeneration; axons reach to the distal edge of the irradiated tissue. Tails shown in A-E are 72 hpa; those in F-G are 7 dpa.

The V-ATPase: endogenous source of H^+ flux required for regeneration

The V-ATPase was suggested as a high-priority candidate in regeneration through a drug screen (Adams and Levin, 2006a; Adams and Levin, 2006b). A wide range of channel/pump blockers had no effect on this process (see Table S1 in the supplementary material). By contrast, V-ATPase blockade, using a highly-specific drug inhibitor or an even more specific molecular dominant-negative subunit, blocked regeneration (Fig. 1B,B′,E), but had no effect on wound healing, normal continued development or tail growth, and did not induce additional apoptosis (Fig. 1C,D). These loss-of-function data, showing inhibition of regeneration but not overall toxicity, confirm the vital role of the V-ATPase in tail regeneration, demonstrate that the regeneration process is not generally labile under pharmacological perturbation, and strongly suggest that it is not simply a housekeeping function necessary for cell survival that is being disrupted by inhibiting V-ATPase.

Although the V-ATPase provides the endogenous ion flux necessary for regeneration, it is the H^+ pumping per se, and not some other function of this complex, that is important, because a heterologous cell membrane H^+ pump was able to rescue regeneration during pharmacologic or physiologic V-ATPase inhibition (Fig. 1F-H). The V-ATPase in the bud cells is localized to the plasma membrane (Fig. 2C″) and, like the PMA pump that rescues refractory embryos, contributes to transmembrane voltage. Inhibition of regeneration with a reagent that depolarizes strongly but does not produce a pH gradient (PTX) suggests that the voltage contribution of H^+ transport activity is crucial. As in the early frog embryo (Adams et al., 2006), the bud-localization and cell-membrane H^+ pump rescue data indicate that it is the cell-surface activity of this pump that is key. This does not rule out the possibility that the voltage across internal membranes is also controlled in part by the V-ATPase; however, PMA's ability to rescue regeneration while localized specifically in the plasma membrane argues that plasma membrane voltage is crucial for regeneration.

Concanamycin inhibits regeneration during the first 24 hours of regeneration, but not prior to amputation (during primary tail development). Together with the results that normal development of the rest of the tail and continued normal development of anterior tissues after tail amputation are unaffected by concanamycin, this argues for a regeneration-specific role of V-ATPase; it also argues against any relevance of early effects our constructs might have had when injected during cleavage stages. Moreover, the effects on regeneration (loss- and gain-of-function) specifically occurred in those animals in which the early expression of a co-injected reporter was observed in the tail prior to cutting. Together with a rapid, endogenous upregulation of plasma-membrane V-ATPase in wound cells (Fig. 2B-C″) and V-ATPase-dependent membrane voltage changes in the regeneration bud (Fig. 3), this argues for a role at the site of regeneration starting between 6 and 12 hpa.

Induction of regeneration by H^+ flow

H^+ pumping is sufficient for inducing regeneration because a heterologous H^+ pump is able to substitute for V-ATPase (Fig. 1G,G′,H; Fig. 3I′-J′). Although in unmanipulated tails this H^+ pumping activity is normally provided by V-ATPase, it can be mimicked by other means of H^+ extrusion. It is striking that the expression of a single H^+ pump can overcome inhibitory conditions, and this suggests that H^+ flux is upstream of regeneration pathways that are not disabled during the refractory period, but, rather, are simply not triggered. A primary role for ion transport in the wound epithelium is consistent with classical transplantation studies revealing that it is the skin that determines the regeneration potential in limbs (Borgens, 1984; Rose and Seller, 1946; Slack, 1980). Although we have shown that V-ATPase function is required for regeneration, mere V-ATPase expression is not sufficient to induce regeneration, as refractory tails still express V-ATPase in the bud (Fig. 2D) but are unable to regenerate (Fig. 3G′,G″). It is likely that the 'refractory' condition involves yet-uncharacterized post-translational factors that interfere with V-ATPase's ability to repolarize the bud. Importantly, our data indicate that the yeast P-type H^+ pump is able to overcome these non-permissive conditions (Fig. 5E′) and is thus a good candidate for use as a reagent to manipulate cell membrane voltage in other systems subject to a time-dependent loss of regenerative ability. The demonstrated rescue of the patterning of axon growth (Fig. 5A-G) reveals that the H^+

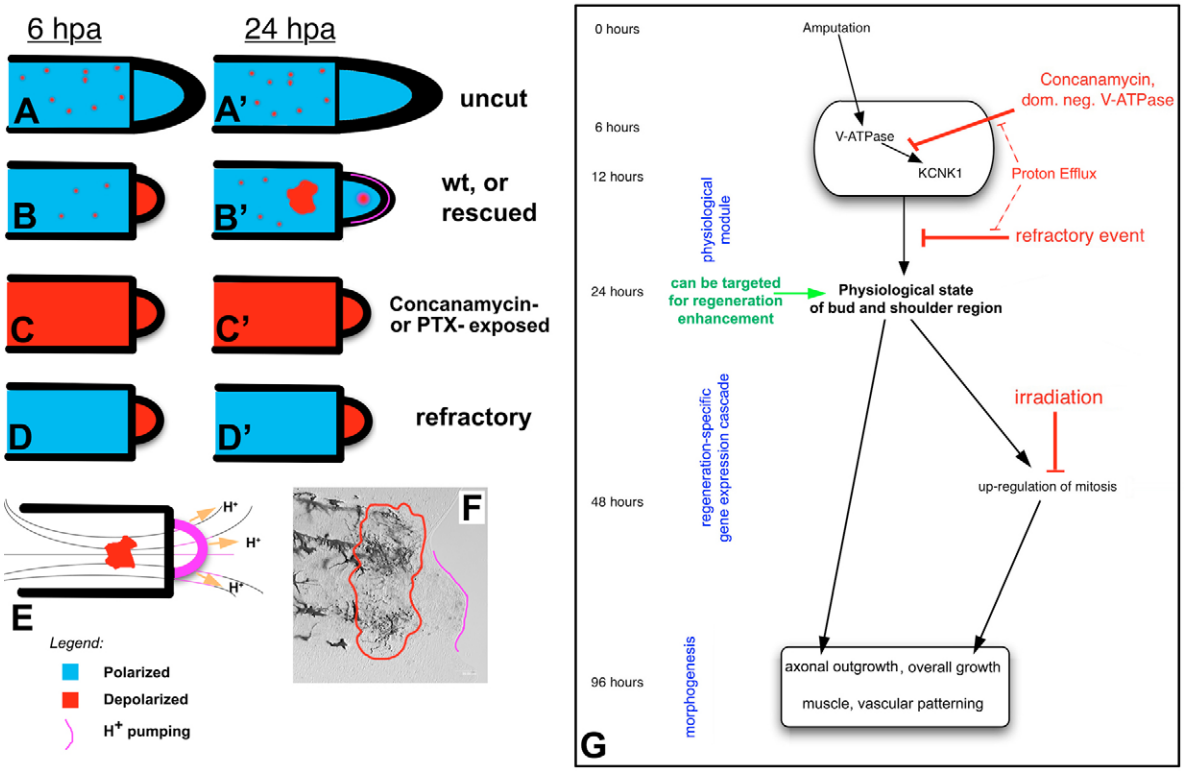

Fig. 6. A biophysical model of the mechanisms controlling tail regeneration. (**A-F**) Schematics of the physiological events occurring in tails under different conditions. The intact tail (A,A′) is generally hyperpolarized, with a distributed pattern of depolarized cells. The regenerating tail exhibits a bud that is first depolarized (B) but is then repolarized by the normal expression of the V-ATPase or induced expression of the PMA H^+-pump (B′); by 24 hpa, a depolarized cell group has appeared in the center of the trunk just anterior to the bud (the 'shoulder region'). (C) V-ATPase-inhibited, or PTX-treated, tails are fully depolarized and are not able to repolarize the bud by 24 hpa (C′). (D,D′) Refractory tails are likewise unable to repolarize the bud and do not possess a depolarized cell group in the shoulder region. (E) Thus, the tail possesses two separate biophysical components: a transepithelial potential normally driven by proton-extruder expression at the edge [likely to result in an electric field (curved lines) that may guide axons into the bud], and a population of cells in the shoulder region that becomes depolarized in tails capable of regenerating. (F) The significance of the shoulder region is unknown, but it may be a region of highly active morphogenesis, as evidenced by the disorganization of the mature melanocytes in this region. (**G**) A step-wise model of tail regeneration consisting of physiological, gene expression and morphogenetic modules. Amputation triggers a cassette of ion transporter expression in existing cells, with V-ATPase expressed as early as 6 hpa and inducing KCNK1 (12-24 hpa). This results in a particular pattern of relative hyper- and depolarization in the regeneration bud and shoulder cells, respectively (characterized at 24 hpa in Fig. 3). A key parameter here is the physiological condition of bud cells (membrane voltage); when hyperpolarized by the activity of a H^+ pump, whether naturally or through judicious misexpression of specific transporters, this leads to depolarization in a rostral cell group (24 hpa), an upregulation of mitosis (48 hpa), and subsequent axonal outgrowth (48-72 hpa), ultimately resulting in the regeneration of the complete tail. Refractory-stage larvae cannot regenerate owing to a failure to repolarize the bud and depolarize shoulder region cells. Ectopically-induced H^+ flux can rescue upstream steps and initiate the program of regeneration, thus representing a tractable initiation point for therapeutic approaches.

pumping provides not merely a permissive yes/no signal, but also contributes a degree of morphogenetic information to neuronal cells.

Physiological domains responsible for regenerative ability in the tail

The direct spatial characterization of electrophysiology of the tail under various conditions (Fig. 3) revealed two bioelectrically unique regions (Fig. 6A-F). Firstly, the regeneration bud expresses V-ATPase, and its activity is revealed by the hyperpolarization of the bud under regeneration-permissive conditions. This extrusion of positive charges at the bud surface would produce the well-studied trans-epithelial potential (McCaig et al., 2005), which is known to guide migratory cells during morphogenesis (Shi and Borgens, 1995; Zhao et al., 2006). The other special region is present in the 'shoulder' anterior to the bud (Fig. 6F); these cells are depolarized under permissive conditions. In light of the known link between depolarization and de-differentiation state (Cone, 1971; Cone and Cone, 1976; Olivotto et al., 1996), it is tempting to hypothesize that the disorganized melanocytes observed there (Fig. 6F) are indicative of a region of active morphogenetic respecification. It is not yet known whether the depolarization of core cells in the shoulder region is due to the electric field arising from transport at the bud (or conventional biochemical signals), but characterization of this region, and the specific transporters underlying its depolarization, are a high priority for future work.

Consistent with a primary role of voltage in regenerative processes (Borgens, 1988; Jenkins et al., 1996; McGinnis and Vanable, 1986), our data show strong differences in membrane-voltage-reporter dye signal among tail cells in conditions of different regenerative ability (Fig. 3). Comparison of voltage maps (Fig. 3E) revealed that regenerating buds must repolarize themselves within

24 hpa. By contrast, under non-growing conditions (Fig. 3E-G′), we observed stronger and/or more depolarization (refractory and V-ATPase-inhibited). This is consistent with a pivotal role for V-ATPase activity in setting the membrane voltage level of bud cells. Uncut tails exhibit a highly variable population of depolarized cells throughout, possibly indicative of the slow distributed growth pattern of intact tails. The voltage of the cells in regenerating tails is set by a different mechanism; H^+ pumping is thus a physiological process that distinguishes regeneration from normal growth and wound healing.

Synthesis of data into a step-wise, mechanistic model of regeneration

We suggest a model that integrates the known molecular genetic and physiological components (Fig. 6G) and is consistent with previous studies linking membrane voltage level to growth and morphogenetic potential in organisms from yeast (Yenush et al., 2002) to mammals (Amigorena et al., 1990; Binggeli and Weinstein, 1986; Cone and Cone, 1976; Cone and Tongier, 1971; Kunzelmann, 2005; Nilius and Wohlrab, 1992; Wang et al., 1998; Woodfork et al., 1995). Amputation triggers expression of the V-ATPase in existing wound cells. The voltage gradient in the bud depends on the V-ATPase, but the precise physiological state is likely to be a complex function of several transporters. K^+ ions are usually key to the control of membrane voltage and could assist in the repolarization function; thus, the KCNK1 channel expressed in the bud downstream of V-ATPase activity represents an important target for future functional analysis.

Downstream of the physiological module driven by H^+ pump activity lies expression of the regeneration-specific genes and, in parallel, upregulation of cell division and neuronal outgrowth – two major components of the regenerative response. How do voltage gradients translate into morphogenetic cues? A variety of biophysical mechanisms for transducing membrane voltage changes to secondary messenger effectors are now known (Cherubini et al., 2005; Levin et al., 2006; Murata et al., 2005). Our data suggest that control of regeneration by V-ATPase-dependent proton flux may take place through at least two mechanisms: control of cell number through modulation of membrane voltage (Cone, 1974; Cone and Cone, 1976; Gilbert et al., 1996; Olivotto et al., 1996; Tseng et al., 2007), and proper guidance of axon growth into the regenerate.

It has long been known that nerve supply is a key factor in regeneration (Bodemer, 1964; Singer, 1952; Thornton, 1956; Yntema, 1959). The observation that neurites are galvanotactic (Hinkle et al., 1981; McCaig, 1986; McCaig et al., 2002; Pullar et al., 2001; Trollinger et al., 2000) and that applied fields induce hyper-innervation of treated limbs led several investigators to hypothesize that regeneration bud currents induce regeneration by attracting migratory neuronal cells (Hanson and McGinnis, 1994; Politis and Zanakis, 1988). Although gradients of membrane voltage per se will not induce galvanotaxis, the H^+ flux from V-ATPases functioning in the bud epithelium (Fig. 2C) creates an electric field (Fig. 6E) that may lead to large-scale bioelectric conditions that trigger galvanotaxis of neurons (Gruler and Nuccitelli, 1991; McCaig et al., 2002). However, it is unlikely that induction of axonal growth by ion transport is the only mechanism required because, in the PMA rescue experiments, many more tails exhibited rescued axon growth (83%) than exhibited regeneration (36%).

Our observations reveal a hitherto unidentified molecular component of regeneration that functions alongside the important recently discovered biochemical controls of this process (Slack et al., 2004). The efficiency of the induction of regeneration might be improved even further by future work that gained a finer control over ion flow in the bud and shoulder region. To our knowledge, this is the first example of the induction of regeneration by molecular expression of an ion transporter and provides a novel entry-point into this complex process. The membrane voltage gradients and H^+ flows driven by the V-ATPase and other transporters are a promising target for gain-of-function approaches. Genetic modulation of ion flows in existing cells within wounds may be exploited by future biomedical efforts and may be a promising new modality for augmenting regeneration and minimizing side effects in clinical settings.

We thank Dayong Qiu, Punita Koustubhan and Katherine Gallant for technical assistance; C. Masuda and M. Montero-Lomeli for PMA constructs; M. Lu for the YCHE78 construct; Scott Holley for the RFP construct; and Kenneth Ryan and John Gurdon for the GFP construct. We thank Min Zhao, Ken Robinson, Peter Smith, Rich Nuccitelli and Richard Borgens for many useful discussions. This work was supported in part by NHTSA grant DTNH22-06-G-00001 and NIH grant GM-06227 to M.L., and NIH grant K22DE016633 to D.S.A. We gratefully acknowledge the useful comments of anonymous reviewers, and the support and expertise of the BioCurrents Research Center, MBL, Woods Hole, MA (NIH grant P41 RR001395). Part of this investigation was conducted in a Forsyth Institute facility renovated with support from Research Facilities Improvement Grant CO6RR11244 from the National Center for Research Resources, National Institutes of Health.

Supplementary material

Supplementary material for this article is available at
http://dev.biologists.org/cgi/content/full/134/7/1323/DC1

References

Abdel-Karim, A. E., Michael, M. I. and Anton, H. J. (1990). Mitotic activity in the blastema and stump tissues of regenerating hind limbs of Xenopus laevis larvae after amputation at ankle level. An autoradiographic study. *Folia Morphol. Praha* **38**, 1-11.

Adams, D. S. and Levin, M. (2006a). Inverse drug screens: a rapid and inexpensive method for implicating molecular targets. *Genesis* **44**, 530-540.

Adams, D. S. and Levin, M. (2006b). Strategies and techniques for investigation of biophysical signals in patterning. In *Analysis of Growth Factor Signaling in Embryos* (ed. M. Whitman and A. K. Sater), pp. 177-262. Boca Raton: Taylor & Francis.

Adams, D. S., Robinson, K. R., Fukumoto, T., Yuan, S., Albertson, R. C., Yelick, P., Kuo, L., McSweeney, M. and Levin, M. (2006). Early, H+-V-ATPase-dependent proton flux is necessary for consistent left-right patterning of non-mammalian vertebrates. *Development* **133**, 1657-1671.

Amigorena, S., Choquet, D., Teillaud, J. L., Korn, H. and Fridman, W. H. (1990). Ion channel blockers inhibit B cell activation at a precise stage of the G1 phase of the cell cycle. Possible involvement of K^+ channels. *J. Immunol.* **144**, 2038-2045.

Beck, C. W., Christen, B. and Slack, J. M. (2003). Molecular pathways needed for regeneration of spinal cord and muscle in a vertebrate. *Dev. Cell* **5**, 429-439.

Binggeli, R. and Weinstein, R. (1986). Membrane potentials and sodium channels: hypotheses for growth regulation and cancer formation based on changes in sodium channels and gap junctions. *J. Theor. Biol.* **123**, 377-401.

Bodemer, C. W. (1964). Evocation of regrowth phenomena in anuran limbs by electrical stimulation of the nerve supply. *Anat. Rec.* **148**, 441-457.

Borgens, R. B. (1984). Are limb development and limb regeneration both initiated by an integumentary wounding? A hypothesis. *Differentiation* **28**, 87-93.

Borgens, R. B. (1988). Voltage gradients and ionic currents in injured and regenerating axons. *Adv. Neurol.* **47**, 51-66.

Borgens, R. B., Vanable, J. W., Jr and Jaffe, L. F. (1977). Bioelectricity and regeneration. I. Initiation of frog limb regeneration by minute currents. *J. Exp. Zool.* **200**, 403-416.

Borgens, R. B., Vanable, J. W., Jr and Jaffe, L. (1979). Small artificial currents enhance Xenopus limb regeneration. *J. Exp. Zool.* **207**, 217-226.

Borgens, R. B., Blight, A. R., Murphy, D. J. and Stewart, L. (1986). Transected dorsal column axons within the guinea pig spinal cord regenerate in the presence of an applied electric field. *J. Comp. Neurol.* **250**, 168-180.

Borgens, R. B., Blight, A. R. and McGinnis, M. E. (1987). Behavioral recovery induced by applied electric fields after spinal cord hemisection in guinea pig. *Science* **238**, 366-369.

Borgens, R., Robinson, K., Vanable, J. and McGinnis, M. (1989). *Electric Fields in Vertebrate Repair*. New York: Alan R. Liss.

Borgens, R. B., Blight, A. R. and McGinnis, M. E. (1990). Functional recovery after spinal cord hemisection in guinea pigs: the effects of applied electric fields. *J. Comp. Neurol.* **296**, 634-653.

Bowman, E. J., O'Neill, F. J. and Bowman, B. J. (1997). Mutations of pma-1, the

gene encoding the plasma membrane H+-ATPase of Neurospora crassa, suppress inhibition of growth by concanamycin A, a specific inhibitor of vacuolar ATPases. *J. Biol. Chem.* **272**, 14776-14786.
Cadinouche, M. Z., Liversage, R. A., Muller, W. and Tsilfidis, C. (1999). Molecular cloning of the Notophthalmus viridescens radical fringe cDNA and characterization of its expression during forelimb development and adult forelimb regeneration. *Dev. Dyn.* **214**, 259-268.
Cannata, S. M., Bagni, C., Bernardini, S., Christen, B. and Filoni, S. (2001). Nerve-independence of limb regeneration in larval Xenopus laevis is correlated to the level of fgf-2 mRNA expression in limb tissues. *Dev. Biol.* **231**, 436-446.
Castle, N. A. and Strichartz, G. R. (1988). Palytoxin induces a relatively non-selective cation permeability in frog sciatic nerve which can be inhibited by cardiac glycosides. *Toxicon* **26**, 941-951.
Cherubini, A., Hofmann, G., Pillozzi, S., Guasti, L., Crociani, O., Cilia, E., Di Stefano, P., Degani, S., Balzi, M., Olivotto, M. et al. (2005). Human ether-a-go-go-related gene 1 channels are physically linked to beta1 integrins and modulate adhesion-dependent signaling. *Mol. Biol. Cell* **16**, 2972-2983.
Cone, C. D. (1971). Unified theory on the basic mechanism of normal mitotic control and oncogenesis. *J. Theor. Biol.* **30**, 151-181.
Cone, C. D. (1974). The role of the surface electrical transmembrane potential in normal and malignant mitogenesis. *Ann. N. Y. Acad. Sci.* **238**, 420-435.
Cone, C. D. and Cone, C. M. (1976). Induction of mitosis in mature neurons in central nervous system by sustained depolarization. *Science* **192**, 155-158.
Cone, C. D. and Tongier, M. (1971). Control of somatic cell mitosis by simulated changes in the transmembrane potential level. *Oncology* **25**, 168-182.
Deuchar, E. M. (1975). Regeneration of the tail bud in Xenopus embryos. *J. Exp. Zool.* **192**, 381-390.
Douglas, B. S. (1972). Conservative management of guillotine amputation of the finger in children. *Aust. Paediatr. J.* **8**, 86-89.
Duboc, V., Rottinger, E., Lapraz, F., Besnardeau, L. and Lepage, T. (2005). Left-right asymmetry in the sea urchin embryo is regulated by nodal signaling on the right side. *Dev. Cell* **9**, 147-158.
Epps, D., Wolfe, M. and Groppi, V. (1994). Characterization of the steady-state and dynamic fluorescence properties of the potential-sensitive dye bis-(1,3-dibutylbarbituric acid)trimethine oxonol (Dibac4(3)) in model systems and cells. *Chem. Phys. Lipids* **69**, 137-150.
Esser, A. T., Smith, K. C., Weaver, J. C. and Levin, M. (2006). Mathematical model of morphogen electrophoresis through gap junctions. *Dev. Dyn.* **235**, 2144-2159.
Etter, A., Cully, D. F., Liu, K. K., Reiss, B., Vassilatis, D. K., Schaeffer, J. M. and Arena, J. P. (1999). Picrotoxin blockade of invertebrate glutamate-gated chloride channels: subunit dependence and evidence for binding within the pore. *J. Neurochem.* **72**, 318-326.
Gardiner, D. M., Endo, T. and Bryant, S. V. (2002). The molecular basis of amphibian limb regeneration: integrating the old with the new. *Semin. Cell Dev. Biol.* **13**, 345-352.
Gargioli, C. and Slack, J. M. (2004). Cell lineage tracing during Xenopus tail regeneration. *Development* **131**, 2669-2679.
Gasque, G., Labarca, P., Reynaud, E. and Darszon, A. (2005). Shal and shaker differential contribution to the K^+ currents in the Drosophila mushroom body neurons. *J. Neurosci.* **25**, 2348-2358.
Gilbert, M. S., Saad, A. H., Rupnow, B. A. and Knox, S. J. (1996). Association of BCL-2 with membrane hyperpolarization and radioresistance. *J. Cell. Physiol.* **168**, 114-122.
Gruler, H. and Nuccitelli, R. (1991). Neural crest cell galvanotaxis – new data and a novel-approach to the analysis of both galvanotaxis and chemotaxis. *Cell Motil. Cytoskeleton* **19**, 121-133.
Hanson, S. M. and McGinnis, M. E. (1994). Regeneration of rat sciatic nerves in silicone tubes: characterization of the response to low intensity d.c. stimulation. *Neuroscience* **58**, 411-421.
Harland, R. M. (1991). In situ hybridization: an improved whole mount method for *Xenopus* embryos. In *Xenopus laevis: Practical Uses in Cell and Molecular Biology*. Vol. 36 (ed. B. K. Kay and H. B. Peng), pp. 685-695. San Diego: Academic Press.
Hibino, T., Ishii, Y., Levin, M. and Nishino, A. (2006). Ion flow regulates left-right asymmetry in sea urchin development. *Dev. Genes Evol.* **216**, 265-276.
Hilgemann, D. W. (2003). From a pump to a pore: how palytoxin opens the gates. *Proc. Natl. Acad. Sci. USA* **100**, 386-388.
Hinkle, L., McCaig, C. D. and Robinson, K. R. (1981). The direction of growth of differentiating neurons and myoblasts from frog embryos in an applied electric-field. *J. Physiol. Lond.* **314**, 121-135.
Huss, M., Ingenhorst, G., Konig, S., Gassel, M., Drose, S., Zeeck, A., Altendorf, K. and Wieczorek, H. (2002). Concanamycin A, the specific inhibitor of V-ATPases, binds to the Vo subunit c. *J. Biol. Chem.* **277**, 40544-40548.
Illingworth, C. M. (1974). Trapped fingers and amputated finger tips in children. *J. Pediatr. Surg.* **9**, 853-858.
Ishino, T., Shirai, M., Kunieda, T., Sekimizu, K., Natori, S. and Kubo, T. (2003). Identification of genes induced in regenerating Xenopus tadpole tails by using the differential display method. *Dev. Dyn.* **226**, 317-325.
Jenkins, L. S., Duerstock, B. S. and Borgens, R. B. (1996). Reduction of the current of injury leaving the amputation inhibits limb regeneration in the red spotted newt. *Dev. Biol.* **178**, 251-262.
Kerns, J. M. and Lucchinetti, C. (1992). Electrical field effects on crushed nerve regeneration. *Exp. Neurol.* **117**, 71-80.
Kunzelmann, K. (2005). Ion channels and cancer. *J. Membr. Biol.* **205**, 159-173.
Levin, M. (2003). Bioelectromagnetic patterning fields: roles in embryonic development, regeneration, and neoplasm. *Bioelectromagnetics* **24**, 295-315.
Levin, M. (2004). A novel immunohistochemical method for evaluation of antibody specificity and detection of labile targets in biological tissue. *J. Biochem. Biophys. Methods* **58**, 85-96.
Levin, M. and Mercola, M. (1998). Gap junctions are involved in the early generation of left right asymmetry. *Dev. Biol.* **203**, 90-105.
Levin, M., Thorlin, T., Robinson, K. R., Nogi, T. and Mercola, M. (2002). Asymmetries in H^+/K^+-ATPase and cell membrane potentials comprise a very early step in left-right patterning. *Cell* **111**, 77-89.
Levin, M., Buznikov, G. A. and Lauder, J. M. (2006). Of minds and embryos: left-right asymmetry and the serotonergic controls of pre-neural morphogenesis. *Dev. Neurosci.* **28**, 171-185.
Li, H. C., Kagami, H., Matsui, K. and Ono, T. (2001). Restriction of proliferation of primordial germ cells by the irradiation of Japanese quail embryos with soft X-rays. *Comp. Biochem. Physiol.* **130A**, 133-140.
Lu, M., Vergara, S., Zhang, L., Holliday, L. S., Aris, J. and Gluck, S. L. (2002). The amino-terminal domain of the E subunit of vacuolar H(+)-ATPase (V-ATPase) interacts with the H subunit and is required for V-ATPase function. *J. Biol. Chem.* **277**, 38409-38415.
Masuda, C. A. and Montero-Lomeli, M. (2000). An NH2-terminal deleted plasma membrane H+-ATPase is a dominant negative mutant and is sequestered in endoplasmic reticulum derived structures. *Biochem. Cell Biol.* **78**, 51-58.
McCaig, C. D. (1986). Electric fields, contact guidance and the direction of nerve growth. *J. Embryol. Exp. Morphol.* **94**, 245-255.
McCaig, C. D., Rajnicek, A. M., Song, B. and Zhao, M. (2002). Has electrical growth cone guidance found its potential? *Trends Neurosci.* **25**, 354-359.
McCaig, C. D., Rajnicek, A. M., Song, B. and Zhao, M. (2005). Controlling cell behavior electrically: current views and future potential. *Physiol. Rev.* **85**, 943-978.
McDevitt, L., Fortner, P. and Pomeranz, B. (1987). Application of weak electric field to the hindpaw enhances sciatic motor nerve regeneration in the adult rat. *Brain Res.* **416**, 308-314.
McGinnis, M. E. and Vanable, J. W., Jr (1986). Voltage gradients in newt limb stumps. *Prog. Clin. Biol. Res.* **210**, 231-238.
Murata, Y., Iwasaki, H., Sasaki, M., Inaba, K. and Okamura, Y. (2005). Phosphoinositide phosphatase activity coupled to an intrinsic voltage sensor. *Nature* **435**, 1239-1243.
Nieuwkoop, P. D. and Faber, J. (1967). Normal table of *Xenopus laevis* (Daudin). Amsterdam: North-Holland.
Nilius, B. and Wohlrab, W. (1992). Potassium channels and regulation of proliferation of human melanoma cells. *J. Physiol.* **445**, 537-548.
Nishi, T. (2002). The vacuolar (H+)-ATPases–nature's most versatile proton pumps. *Nat. Rev. Mol. Cell Biol.* **3**, 94-103.
Nuccitelli, R. (1988). Ionic currents in morphogenesis. *Experientia* **44**, 657-666.
Olivotto, M., Arcangeli, A., Carla, M. and Wanke, E. (1996). Electric fields at the plasma membrane level: a neglected element in the mechanisms of cell signalling. *BioEssays* **18**, 495-504.
Politis, M. J. and Zanakis, M. F. (1988). Treatment of the damaged rat hippocampus with a locally applied electric field. *Exp. Brain Res.* **71**, 223-226.
Politis, M. J., Zanakis, M. F. and Albala, B. J. (1988). Mammalian optic nerve regeneration following the application of electric fields. *J. Trauma* **28**, 1548-1552.
Pullar, C. E., Isseroff, R. R. and Nuccitelli, R. (2001). Cyclic AMP-dependent protein kinase a plays a role in the directed migration of human keratinocytes in a DC electric field. *Cell Motil. Cytoskeleton* **50**, 207-217.
Pyza, E., Borycz, J., Giebultowicz, J. M. and Meinertzhagen, I. A. (2004). Involvement of V-ATPase in the regulation of cell size in the fly's visual system. *J. Insect Physiol.* **50**, 985-994.
Robinson, K. R. and Messerli, M. A. (2003). Left/right, up/down: the role of endogenous electrical fields as directional signals in development, repair and invasion. *BioEssays* **25**, 759-766.
Rose, S. M. and Seller, C. J. (1946). Type of regeneration in limbs of frogs after transplantation of adult skin. *Anat. Rec.* **94**, 415.
Ryffel, G. U., Werdien, D., Turan, G., Gerhards, A., Goosses, S. and Senkel, S. (2003). Tagging muscle cell lineages in development and tail regeneration using Cre recombinase in transgenic Xenopus. *Nucleic Acids Res.* **31**, e44.
Saka, Y. and Smith, J. C. (2001). Spatial and temporal patterns of cell division during early Xenopus embryogenesis. *Dev. Biol.* **229**, 307-318.
Salo, E. and Baguna, J. (1985). Cell movement in intact and regenerating planarians. Quantitation using chromosomal, nuclear and cytoplasmic markers. *J. Embryol. Exp. Morphol.* **89**, 57-70.

Sanchez Alvarado, A. (2003). The freshwater planarian Schmidtea mediterranea: embryogenesis, stem cells and regeneration. *Curr. Opin. Genet. Dev.* **13**, 438-444.
Shapiro, S., Borgens, R., Pascuzzi, R., Roos, K., Groff, M., Purvines, S., Rodgers, R. B., Hagy, S. and Nelson, P. (2005). Oscillating field stimulation for complete spinal cord injury in humans: a phase 1 trial. *J. Neurosurg. Spine* **2**, 3-10.
Shi, R. and Borgens, R. B. (1995). Three-dimensional gradients of voltage during development of the nervous system as invisible coordinates for the establishment of embryonic pattern. *Dev. Dyn.* **202**, 101-114.
Shimeld, S. M. and Levin, M. (2006). Evidence for the regulation of left-right asymmetry in *Ciona intestinalis* by ion flux. *Dev. Dyn.* **235**, 1543-1553.
Singer, M. (1952). The influence of the nerve in regeneration of the amphibian extremity. *Q. Rev. Biol.* **27**, 169-200.
Sive, H. L., Grainger, R. M. and Harland, R. M. (2000). *Early Development of Xenopus laevis*. Cold Spring Harbor: Cold Spring Harbor Laboratory Press.
Slack, J. M. W. (1980). Morphogenetic properties of the skin in axolotl limb regeneration. *J. Embryol. Exp. Morphol.* **58**, 265-288.
Slack, J. M. W., Beck, C. W., Gargioli, C. and Christen, B. (2004). Cellular and molecular mechanisms of regeneration in Xenopus. *Philos. Trans. R. Soc. Lond. B Biol. Sci.* **359**, 745-751.
Sugiura, T., Taniguchi, Y., Tazaki, A., Ueno, N., Watanabe, K. and Mochii, M. (2004). Differential gene expression between the embryonic tail bud and regenerating larval tail in Xenopus laevis. *Dev. Growth Differ.* **46**, 97-105.
Tassava, R. A. (2004). Forelimb spike regeneration in Xenopus laevis: testing for adaptiveness. *J. Exp. Zoolog. Part A Comp. Exp. Biol.* **301**, 150-159.
Tazaki, A., Kitayama, A., Terasaka, C., Watanabe, K., Ueno, N. and Mochii, M. (2005). Macroarray-based analysis of tail regeneration in Xenopus laevis larvae. *Dev. Dyn.* **233**, 1394-1404.
Thornton, C. S. (1956). *Regeneration in Vertebrates*. Chicago: University of Chicago Press.
Tosteson, M. T., Scriven, D. R., Bharadwaj, A., Arnadottir, J. and Tosteson, D. C. (1997). Interactions of palytoxin with the Na,K-ATPase. Where are those sites? *Ann. N. Y. Acad. Sci.* **834**, 424-425.
Tosteson, M. T., Thomas, J., Arnadottir, J. and Tosteson, D. C. (2003). Effects of palytoxin on cation occlusion and phosphorylation of the (Na^+,K^+)-ATPase. *J. Membr. Biol.* **192**, 181-189.
Trollinger, D. R., Isseroff, R. R. and Nuccitelli, R. (2002). Calcium channel blockers inhibit galvanotaxis in human keratinocytes. *J. Cell. Physiol.* **193**, 1-9.
Tseng, A. S., Adams, D. S., Qiu, D., Koustubhan, P. and Levin, M. (2007). Apoptosis is required during early stages of tail regeneration in Xenopus laevis. *Dev. Biol.* **301**, 62-69.
Wang, S., Melkoumian, Z., Woodfork, K. A., Cather, C., Davidson, A. G., Wonderlin, W. F. and Strobl, J. S. (1998). Evidence for an early G1 ionic event necessary for cell cycle progression and survival in the MCF-7 human breast carcinoma cell line. *J. Cell. Physiol.* **176**, 456-464.
Wieczorek, H., Brown, D., Grinstein, S., Ehrenfeld, J. and Harvey, W. R. (1999). Animal plasma membrane energization by proton-motive V-ATPases. *BioEssays* **21**, 637-648.
Woodfork, K. A., Wonderlin, W. F., Peterson, V. A. and Strobl, J. S. (1995). Inhibition of ATP-sensitive potassium channels causes reversible cell-cycle arrest of human breast cancer cells in tissue culture. *J. Cell. Physiol.* **162**, 163-171.
Yenush, L., Mulet, J. M., Arino, J. and Serrano, R. (2002). The Ppz protein phosphatases are key regulators of K^+ and pH homeostasis: implications for salt tolerance, cell wall integrity and cell cycle progression. *EMBO J.* **21**, 920-929.
Yntema, C. L. (1959). Blastema formation in sparsely innervated and aneurogenic forelimbs of amblystoma larvae. *J. Exp. Zool.* **142**, 423-439.
Zernicka-Goetz, M., Pines, J., Ryan, K., Siemering, K. R., Haseloff, J., Evans, M. J. and Gurdon, J. B. (1996). An indelible lineage marker for Xenopus using a mutated green fluorescent protein. *Development* **122**, 3719-3724.
Zhao, M., Song, B., Pu, J., Wada, T., Reid, B., Tai, G., Wang, F., Guo, A., Walczysko, P., Gu, Y. et al. (2006). Electrical signals control wound healing through phosphatidylinositol-3-OH kinase-gamma and PTEN. *Nature* **442**, 457-460.